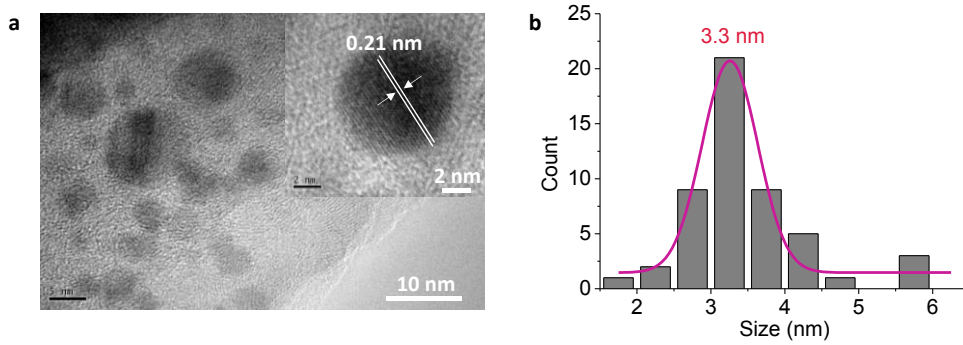


Supporting Information for

**Catalytic route electrochemiluminescence microscopy of cell membranes with nitrogen-doped carbon dots as nano-coreactants**

Cheng Ma, Min-Xuan Wang, Hui-Fang Wei, Shaojun Wu, Jian-Rong Zhang, Jun-Jie Zhu and Zixuan Chen\*

State Key Laboratory of Analytical Chemistry for Life Science, School of Chemistry and Chemical Engineering, Nanjing University, Nanjing 210023, P. R. China.



**Figure S1.** Morphological properties of NCDs. (a) High-resolution TEM image of NCDs. Inset shows the lattice spacing of 0.21 nm in NCDs, which is attributed to the (100) facet of graphite carbon.<sup>1</sup> (b) The statistic size distribution of NCDs.

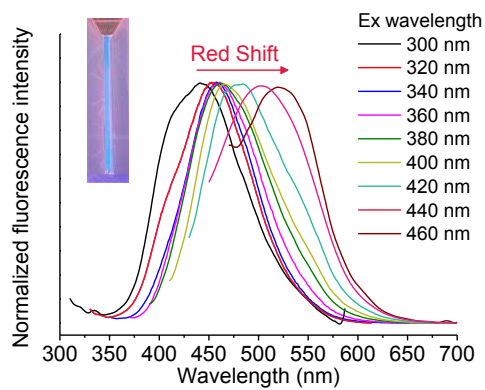


**Figure S2.** Normalized fluorescence spectra of NCDs at different excitation wavelength. The fluorescence spectra show a gradually red shift with the change of excitation wavelength from 300 nm to 460 nm. Inset: photograph of NCDs aqueous solution under 365 nm UV light.

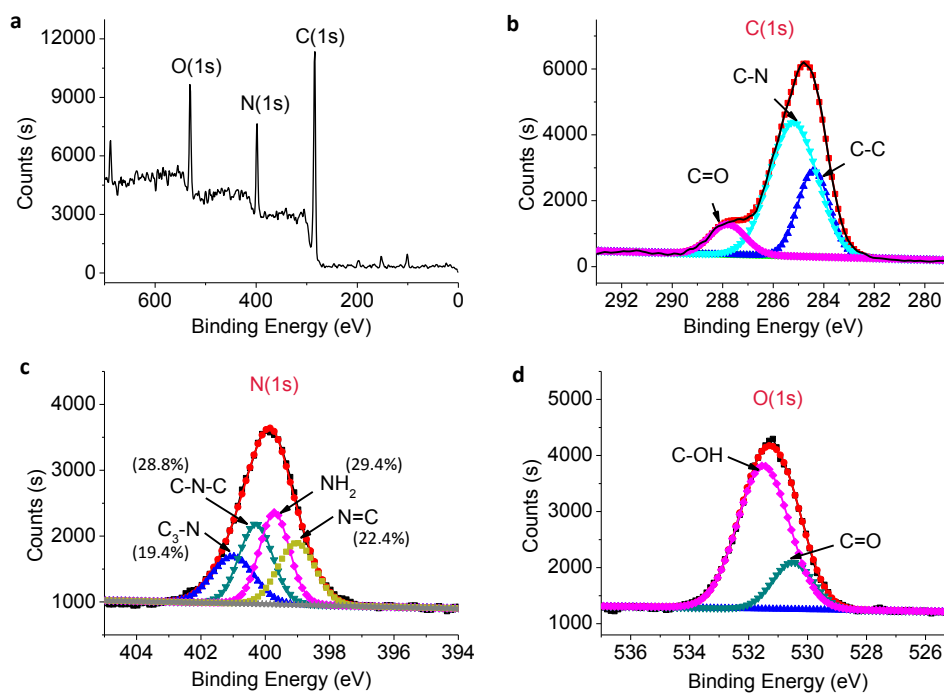


**Figure S3.** (a) The wide XPS spectrum of C(1s), N(1s), O(1s) of NCDs. (b) De-convoluted high resolution XPS spectra for C(1s). (c) De-convoluted high resolution XPS spectra for N(1s). According to the integration areas, the contents of N-C<sub>3</sub>, N-C<sub>2</sub>, NH<sub>2</sub>, and C=N are calculated to be 19.4, 28.8, 29.4, and 22.4%, respectively. (d) De-convoluted high resolution XPS spectra for O(1s).

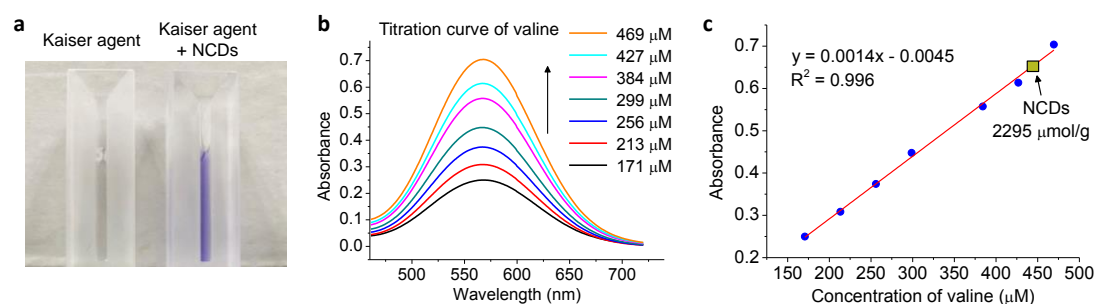


**Figure S4.** The absorbance at 566 nm (blue colour) of Kaiser agent confirms the amino groups on the surface of NCDs.<sup>2</sup> (a) Photographs of Kaiser agent in the absence (left) and presence (right) of NCDs. (b) Absorption spectra of Kaiser agent in the presence of different amounts of valine. The arrow indicates that the signal rises as the concentration of valine increases. Because one valine molecule has only one amino, we obtain the linear correlation equation between the amino amount and the absorbance at 566 nm. (c) Absorbance (at 566 nm) of Kaiser agent as a function of the concentration of valine. According to the absorbance (at 566 nm) of NCDs (the yellow square on the line), the amount of amino groups in NCDs was determined (2295 μmol/g) by the standard linear relation.

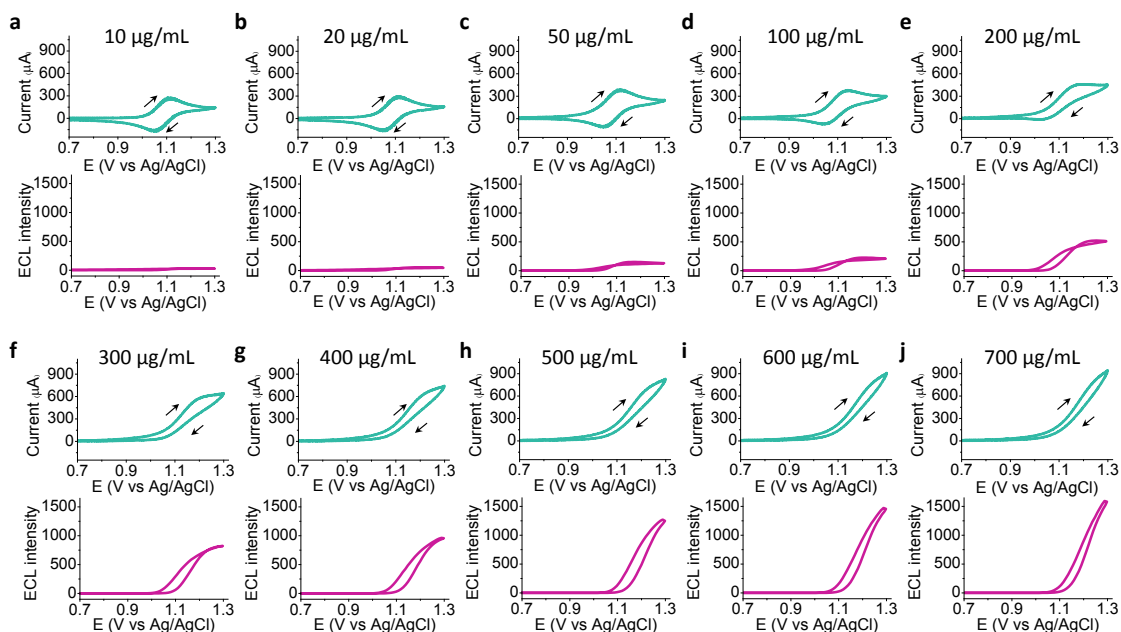


**Figure S5.** (a-j) Cyclic voltammetry curves (cyan lines) and corresponding ECL-potential curves (purple lines) in the PBS buffer (pH = 7.4) containing 10 mM  $\text{Ru}(\text{bpy})_3^{2+}$  and different concentrations of NCDs from 10  $\mu\text{g}/\text{mL}$  to 700  $\mu\text{g}/\text{mL}$ . Scan rate is 0.1 V/s. Work electrode is ITO.

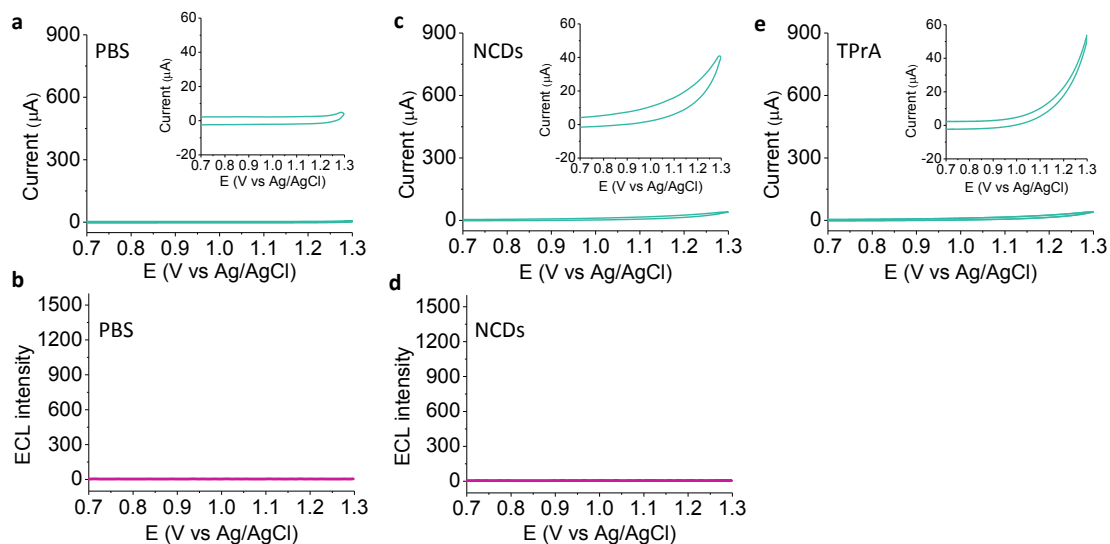


**Figure S6.** (a,b) Cyclic voltammetry curves (cyan lines) and corresponding ECL-potential curves (purple lines) in the PBS buffer (pH = 7.4). (c,d) Cyclic voltammetry curves (cyan lines) and corresponding ECL-potential curves (purple lines) in the PBS buffer (pH = 7.4) containing 1 mg/mL NCDs. (e) Cyclic voltammetry curves in the PBS buffer (pH = 7.4) containing 1 mM TPrA. Scan rate is 0.1 V/s. Work electrode is ITO.

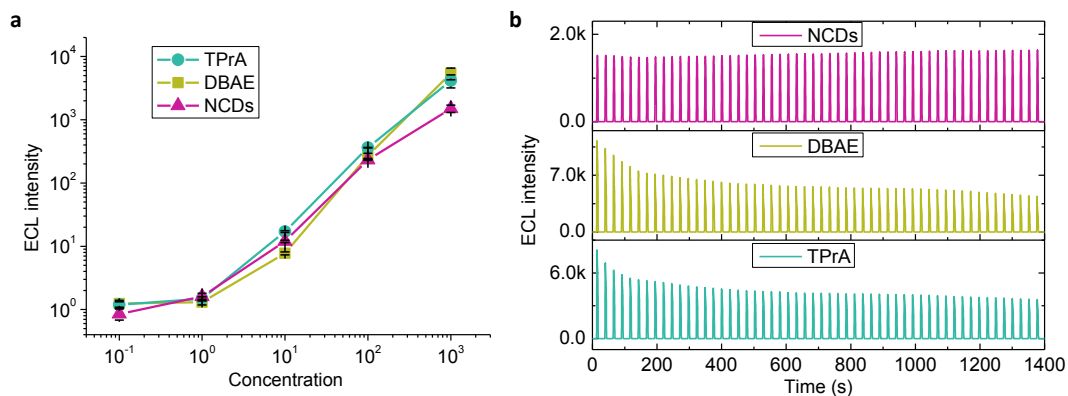


**Figure S7.** (a) Dependence of the ECL peak intensity on the concentrations of TPrA, DBAE, and NCDs as the coreactants of  $\text{Ru}(\text{bpy})_3^{2+}$ . The concentration units of TPrA and DBAE are  $\mu\text{mol/L}$ . The concentration unit of NCDs is  $\mu\text{g/mL}$ . (b) Stability of the ECL intensity of  $\text{Ru}(\text{bpy})_3^{2+}$  using NCDs (1 mg/mL), DBAE (1 mM), and TPrA (1 mM) as coreactants. The potential is cyclically scanned from 0 V to 1.3 V. Scan rate is 0.1 V/s. Work electrode is ITO.

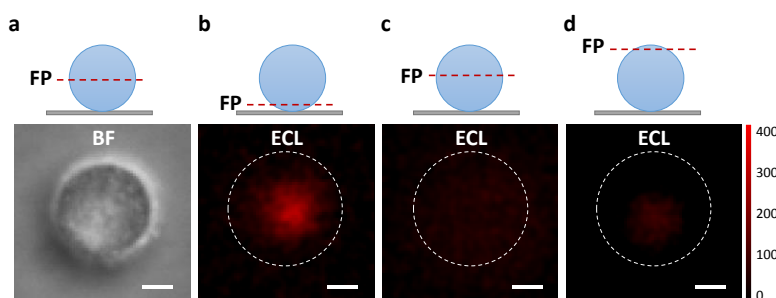


**Figure S8.** (a-d) Bright field (BF) image and corresponding ECL images (exposure time 1 s) of a single bead ( $10\ \mu\text{m}$ ) at different focal planes (FP). The beads were modified with  $\text{Ru}(\text{bpy})_3^{2+}$  via amido bond. The dash line represents the outline of the bead. The work electrode is glassy carbon electrode. ECL imaging was performed in the electrolyte containing 100 mM TPrA as the coreactant. Scale bar (white) is  $3\ \mu\text{m}$ .

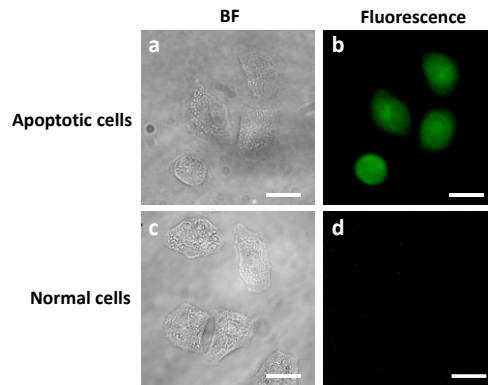


**Figure S9.** Bright field (BF) image (a) and fluorescence image (b) of apoptotic HeLa cells induced by lipopolysaccharide (5  $\mu\text{g}/\text{mL}$ ) for 2 h and then incubated with Annexin V-FITC, a commercial fluorescent detection kit for phosphatidylserine. Bright field image (c) and fluorescence image (d) of normal HeLa cells incubated with Annexin V-FITC. Scale bar (white) is 20  $\mu\text{m}$ .

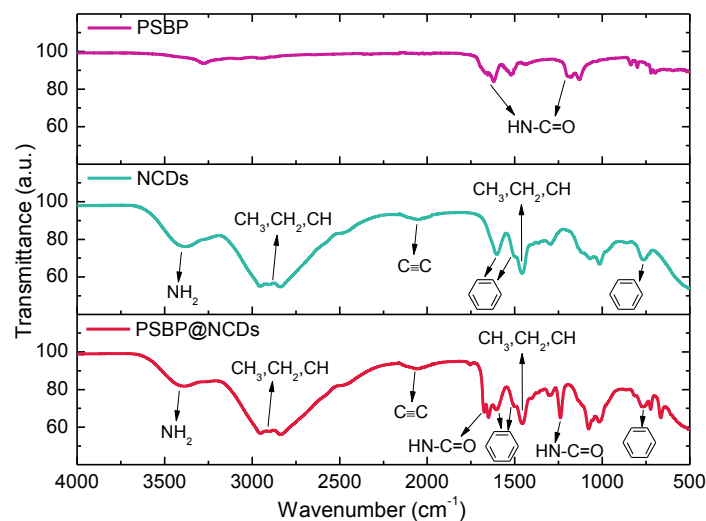


**Figure S10.** FT-IR analysis of PSBP peptide, NCDs, and PSBP@NCDs. For PSBP (purple line), the characteristic absorption peaks for the stretching vibration of HN-C=O in peptide appears at 1622 and 1207  $\text{cm}^{-1}$ . NCDs (cyan line) contain absorption peaks of N-H (3406  $\text{cm}^{-1}$ ) and C-H (2930 and 1461  $\text{cm}^{-1}$ ) inherited from the precursor PEI. Besides, the characteristic absorption peaks of C=C (2060  $\text{cm}^{-1}$ ) and aromatic ring (1607, 1511 and 766  $\text{cm}^{-1}$ ) demonstrate the formation of aromatic ring structure in NCDs. After the conjugation between NCDs and PSBP via amido bond (PSBP@NCDs) (red line), the characteristic absorption peaks from both PSBP and NCDs are observed in the IR spectrum of PSBP@NCDs. It demonstrates the successful conjugation between PSBP and NCDs.

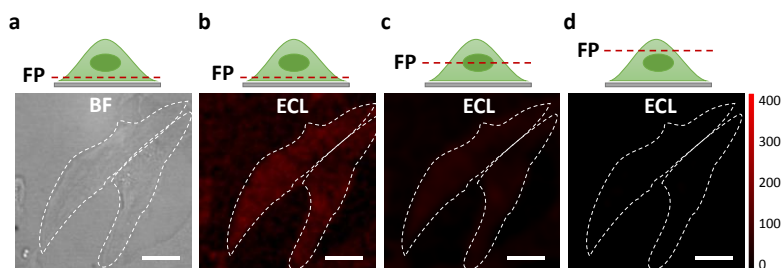


**Figure S11.** (a-d) Bright field (BF) image and corresponding ECL images (exposure time 1 s) of cells at different focal planes (FP). The cells were fixed by by paraformaldehyde for 30 min, treated with 0.1% Triton X-100 for 10 min, and modified with  $\text{Ru}(\text{bpy})_3^{2+}$  via amido bond. Scale bar (white) is 15  $\mu\text{m}$ . The dash line represents the outline of the cell. The work electrode is glassy carbon electrode. ECL imaging was performed in the electrolyte containing 100 mM TPrA as the coreactant.

### Experimental section.

Unless otherwise stated, all the other chemicals and reagents used in this study were of analytical grade quality and were used as received without further purification. Ultrapure water with a resistivity of 18.2  $\text{M}\Omega\ \text{cm}$  was produced by using a Milli-Q apparatus (Millipore) and used in the preparation of all solutions. PDMS was prepared by using Sylgard 184, Dow Corning. Tris(2,2'-bipyridyl)dichlororuthenium(II) hexahydrate ( $\text{Ru}(\text{bpy})_3^{2+}$ ), tripropylamine (TPrA), 2-(dibutylamino)ethanol (DBAE), Kaiser test kit, ethyl(dimethylaminopropyl) carbodiimide (EDC), N-hydroxysuccinimide (NHS), lipopolysaccharides (LPS) from *Escherichia coli* were purchased from Sigma-Aldrich. Annexin V-FITC assay kit and 4% paraformaldehyde solution were purchased from KeyGEN BioTECH. L-valine, succinic acid and branched polyethyleneimine (PEI, MW = 600) were purchased from Aladdin Reagent Inc. Peptide (FNFRLKAGAKIRFGRC, PSBP, 95%) was purchased from Jill Biochemical Co., Ltd. (China). Carboxylate-modified polystyrene bead (10  $\mu\text{m}$ ) were purchased from Macklin Reagent Inc. ITO was purchased from Zhongjingkeyi Technology Co., Ltd. A HeLa cell line were purchased from the Institute of Cell Biology at the Chinese Academy of Sciences (Shanghai, P. R. China) and cultured in HDMEM (Life Technologies, Grand Island, NY, USA) containing 10% fetal bovine serum, 100 U/mL penicillin and 100  $\mu\text{g}/\text{mL}$  streptomycin at 37  $^\circ\text{C}$  under 5%  $\text{CO}_2$  atmosphere. At the logarithmic growth phase, the cells were transferred at an ITO electrode surface and left undisturbed for 8 h for cells adherence. The smooth surface of ITO electrode allowed HeLa cells to adhere to and grow on it.

Fluorescence spectra measurements were conducted on a RF-5301PC fluorescence spectrometer (Shimadzu Co. Japan) equipped with a xenon lamp. Transmission electron micrographs (TEM) were measured on a JEOL JEM 200CX transmission electron microscope using an accelerating voltage of 200 kV. X-ray photoelectron spectroscopy analyses were performed using an ESCALAB 250Xi spectrophotometer (Thermo Fisher Co., USA). Ultraviolet-visible (UV-vis) absorption spectra were obtained using a UV-3600 spectrophotometer (Shimadzu). A Vector 22 spectrometer (Bruker Corporation, America) was applied to obtain the Fourier transform infrared spectroscopy (FT-IR) spectra. The ECL measurements were carried out on a MPI-E detection system (Xi'an Remex, China) with a three-electrode system. The image analysis and processing were performed by Matlab and ImageJ softwares.

### Synthesis of NCDs.

NCDs were synthesized with classic hydrothermal method.<sup>3</sup> Briefly, aqueous solution of 10 mL PEI (280 mg/mL) was transferred into a 50 mL Teflon-lined stainless steel autoclave and then heated at 180°C for 4 h. When cooled down to room temperature, the sample was purified through dialysis against distilled water using dialysis membranes (MWCO = 10 kDa) for 3 days. The collected product was lyophilized and stored at 4°C.

### Synthesis of PSBP@NCDs.

The as-prepared NCDs (0.1 mg/mL, 1 mL) were incubated with a mixture containing 2  $\mu$ M 1-ethyl-3-(3-(dimethylamino)propyl)carbodiimide (EDC), 2  $\mu$ M N-hydroxysuccinimide (NHS), 200 nM succinic acid and 200 nM PSBP for 12 h at 37 °C. Then the sample was purified through dialysis against distilled water using dialysis membranes (MWCO = 10 kDa) for 3 days. The collected product was lyophilized and stored at 4°C.

### Synthesis of polystyrene microbeads (10 $\mu$ m in diameter) modified with NCDs.

Carboxylate-modified polystyrene beads (10 mg/mL, 1 mL) were incubated with a mixture containing 20 mM 1-ethyl-3-(3-(dimethylamino)propyl)carbodiimide (EDC) and 20 mM N-hydroxysuccinimide (NHS) for 2 h at room temperature. Then, 500  $\mu$ L of 1 mg/mL NCDs was reacted with the activated carboxylate-modified polystyrene beads at 37 °C for 12 h. Afterward, the polystyrene beads were centrifuged at 1000 rpm for 3 min and then washed with deionized water.

The detailed ECL microscopy setup has been described previously.<sup>4</sup> Briefly, the ECL microscopy setup was based on a homemade upright configuration microscope and electrochemical workstation, shown below (Figure S10). The microscope was equipped with a numerical aperture (NA = 1.10) water-immersion objective (Olympus LUMFLN x60) and EMCCD camera (Photometrics, Evolve 512 Delta) for increasing spatial resolution and imaging sensitivity, respectively. The high-magnification zoom lens systems in front of the EMCCD camera was set to maximum 4.5X to offer a zoom-in vision. In the electrochemical module, electrochemical workstation provided various techniques to control the electrode potential with a three-electrode system including an Ag/AgCl (saturated KCl) reference electrode, a Pt wire counter electrode, and an ITO work electrode. The three-electrode system was mounted under the objective and regulated by a two-axis linear translation stage with rotating platform. With the constant injection of the electrolyte into the electrochemical cell until both the ITO electrode surface and the water-immersion objective were immersed into the electrolyte, the reference electrode and counter electrode were put in the electrochemical cell from the side. The EMCCD camera was triggered by the potentiostat by a TTL signal.

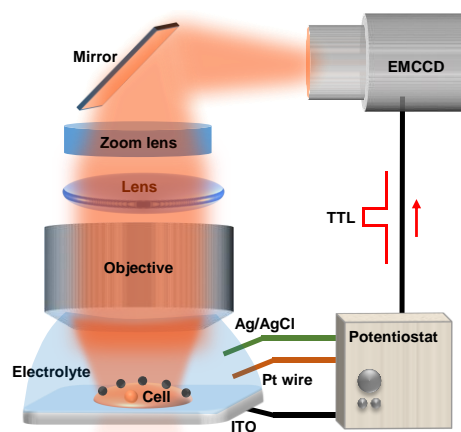


**Figure S12.** Schematic illustration of the ECL microscopy.



## References

1. Y.-S. He, C.-G. Pan, H.-X. Cao, M.-Z. Yue, L. Wang and G.-X. Liang, *Sens. Actuators, B*, 2018, **265**, 371.
2. S. Carrara, F. Arcudi, M. Prato and L. De Cola, *Angew. Chem. Int. Ed.*, 2017, **56**, 4757.
3. B. Han, Y. Li, T. Peng, M. Yu, X. Hu and G. He, *Analytical Methods*, 2018, **10**, 2989.
4. (a) C. Ma, H.-F. Wei, M.-X. Wang, S. Wu, Y.-C. Chang, J. Zhang, L.-P. Jiang, W. Zhu, Z. Chen and Y. Lin, *Nano. Lett.*, 2020, **20**, 5008; (b) C. Ma, S. Wu, Y. Zhou, H.-F. Wei, J. Zhang, Z. Chen, J.-J. Zhu, Y. Lin and W. Zhu, *Angew. Chem. Int. Ed.*, 2020, DOI: 10.1002/anie.202012171.